ISIJ International, Vol. 36 (1996), No. 3, pp. 324–333

Isothermal Transformation Products in a Cu-bearing High Strength Low Alloy Steel

D. P. DUNNE, S. S. GHASEMI BANADKOUKI and D. YU

Department of Materials Engineering, The University of Wollongong, Wollongong, NSW 2522, Australia.

(*Received on August 14, 1995; accepted in final form on November 29, 1995*)

A time-temperature-transformation (TTT) diagram has been determined for a copper-bearing steel, which is a low alloy TMCP variant of the ASTM A710 type of structural steel. Quantitative measurements have been supplemented by optical microscopy and transmission electron microscopy to investigate the isothermal transformation behaviour as well as the associated precipitate morphologies. It is shown that the kinetics and product phases of the polymorphic transformation and precipitation reactions are sensitive to both temperature and time. The TTT-diagram shows a prominent transformation region for bainitic structures, at temperatures intermediate between those of polygonal ferrite and martensite. In the intermediate region, the microstructures were characterised by a ferritic matrix with a lath and/or plate shaped grains containing a high dislocation density, together with a minor dispersed "island" phase. For a short holding time (5 sec) at intermediate temperatures (580–430°C), the island phase was identified as untempered twinned and lath martensite, autotempered twinned and lath martensite, and martensite/austenite constituent, depending on the level of carbon partitioning in the remaining austenite before quenching in water. For a longer holding time, the carbon enriched austenite regions decomposed to carbide and ferrite by coupled growth. Polygonal and quasi-polygonal ferrite were formed at relatively high transformation temperatures and these microstructures contained a low dislocation density and were associated with interphase ε-copper precipitates.

KEY WORDS: Cu-bearing low alloy steel; TTT-diagram; isothermal transformation; granular bainitic; bainitic ferrite; dark islands; interphase precipitation; ε-Cu precipitates.

1. Introduction

Low-carbon copper-bearing age-hardenable high strength low alloy (HSLA) steels are a class of HSLA steel which provide good combinations of strength, low temperature toughness and weldability. They are commonly alloyed with manganese, chromium, molybdenum and nickel.[1–4] Most of the elements provide hardenability for the transformation of austenite to a fine bainitic ("acicular") ferritic microstructure in heavy sections. Consequently, bainite can be produced in heavy sections with little change in tensile properties compared to thinner sections. In addition, the presence of about 1% Cu contributes to precipitate hardening by copper-rich particles during aging,[5–7] as well as promoting good formability,[8] excellent corrosion resistance,[9] and high resistance to fatigue crak growth because of crack path obstacles in the form of fine copper-rich particles.[10] Thus, strength can be achieved without a significant volume fraction of carbide containing microconstituents, and toughness and weldability are enhanced by the low carbon content of the alloys. These engineering properties are capable of meeting the demands of natural gas pipelines, ships, and offshore platforms exposed to Arctic environments.[11,12] Costs are kept low by microalloying, controlling the austenite structure to produce fine ferrite grains and avoiding the need for tempering, particularly in welded structures.[13,14]

Of the commercially available copper-bearing HSLA steels, ASTM A710, which was originally used for the offshore industry, immediately meets the above-mentioned engineering properties without requiring any alloying development or modification. The successful certification program of 80 ksi HSLA steel, based on the ASTM A710 steel system, occurred in early 1984 as a potential replacement for HY80 steel in surface ship hull structural application.[11] In the last few years, application of HSLA80 steel has increased as a substitute for HY80 in cruiser deck, bulkhead and hull applications.[15] However, the microstructural characterisation of these steels is still at an early stage, and so it is the purpose of this paper to describe in detail the microstructures formed in an isothermally transformed, low carbon, Cu-Bearing ASTM A710 type HSLA plate steel. The morphology of primary ferrite grains and the characterisation of associated austenite and martensite regions as a function of isothermal transformation temperature and time are evaluated.

2. Materials and Experimental Procedure

The steel used in the present study was CR HSLA80 steel developed by BHP Steel, SPPD, Port Kembla, Australia. This steel was produced by a thermo-mechanical controlled processing (TMCP) route, with the as received material consisting of a banded ferrite and pearlite structure as shown in **Fig. 1**. The thickness of the plate was 10 mm and the chemical composition is given in **Table 1**.

Specimens were cut into rectangular prisms, $4 \times 10 \times 38\ mm^3$, from the as received steel plate, and a small hole

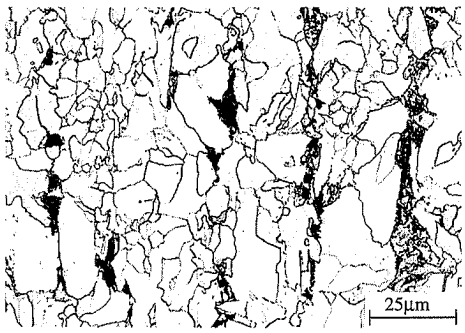

Fig. 1. Optical micrograph of as received hot rolled plate steel (2.5% nital). Longitudinal section containing the rolling direction.

Table 1. Chemical composition (in weight percent) of the CR HSLA80 steel investigated.

C	Mn	Si	Ni	Cu
0.05	1.40	0.25	0.85	1.10
Nb	Ti	P	S	Cr
0.02	0.013	0.012	0.003	—

was drilled at the end of each specimen to locate a thermocouple for recording of the temperature. Specimens were austenitised at 1 200°C for 15 min and then transformed isothermally at a pre-determined temperature and time in a salt bath before water quenching, as shown schematically in **Fig. 2**. To reveal the microstructural constituents of the specimens with sufficient contrast, three different etching reagents were employed, as listed in **Table 2**. The progress of the overall transformation was measured by the point counting method,[16,17] which in some cases was carried out on an MD-20 Image Analyser equipped with a video camera connected to a Nikon optical microscope. Specimens for detailed examination were selected to represent several different types of microstructures.

Specimens transformed isothermally for a selected transformation temperature and time, were examined with transmission electron microscopy (TEM) to ascertain the transformation products, to elucidate details of the ferritic microstructures, as well as the associated copper precipitation at various stages of isothermal transformation. Thin foil specimens were prepared by a twin polishing technique using a solution consisting of 95% acetic acid and 5% perchloric acid. In some cases, the perforated thin foils were ion beam thinned for approximately 3 h at a 9° specimen angle in an Edwards IBT 200 ion beam thinning unit. Observations were carried out in a JEOL 2000 FX operated at 200 kV.

3. Results

3.1. Isothermal Transformation Behaviour

The time-temperature-transformation (TTT) diagram of HSLA80 steel determined by metallographic examination is shown in **Fig. 3**. The temperatures of 760, 610, and 580°C correspond to the equilibrium Ae3, Ae1, and Bs (bainite start) reaction temperatures, respectively. The

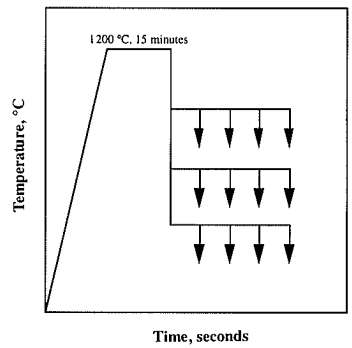

Fig. 2. Schematic isothermal heat treatment procedures.

Table 2. Etching reagents employed.

Etching reagent	Purpose
2.5% Nital	reveals ferrite grain boundaries, differentiates as-quenched low carbon martensite from ferrite
stain etching: solution of aqueous 20% sodium thiosulfate, 2.3% citric acid and 2.3% cadmium chloride	darkens as-quenched high carbon martensite
8 gr sodium metabisulfite + 100 cc distilled water	darkens as-quenched martensite/austenite islands

progress of $\gamma \rightarrow \alpha$ transformation was measured for the start (about 2%), 50 and 80% transformation using quantitative metallography. The data indicated a pro-eutectoid ferrite formation region in the TTT-diagram of 760–600°C, which is significantly depressed because of the presence of the strong austenite stabilising elements Ni, Mn and Cu. Above the Ae1 temperature, the incubation period increased in a typical "C" curve manner with increasing temperature until, at 750°C, only a small volume fraction of decomposition product was detected after 8 h. However, below the Ae1 temperature, the reaction incubation period was found to be very short and this prevented detection of the nose of the curve.

The TTT-diagram also shows a prominent region associated with an intermediate structure, frequently referred to as bainite. This region is shown between the bainite start temperature (Bs) of 580°C and the calculated martensite start temperature (Ms) of 430°C for this steel.[18] The microstructures produced in this region are quite complex and result from the growth of a lath type ferritic structure in association with a second constituent or microphase which can consist of martensite, and/or retained austenite, pearlite, and even carbides, depending upon the supersaturation of carbon in the remaining austenite and the kinetics of carbon diffusion.

An example of bainitic structures (granular bainitic "αB" and bainitic ferrite "α°B") obtained at an intermediate transformation temperature (480°C for 5 sec) is shown in **Fig. 4(a)** and the associated microphase regions are revealed in **Fig. 4(b)**. Assuming that the microstructure is 95% ferrite with a carbon content of 0.02%, a mass balance indicates that the remaining austenite would contain 0.62% carbon. This carbon content corresponds to calculated Ms and Mf temperatures of 210 and 10°C, respectively.[18] This calculation is in-

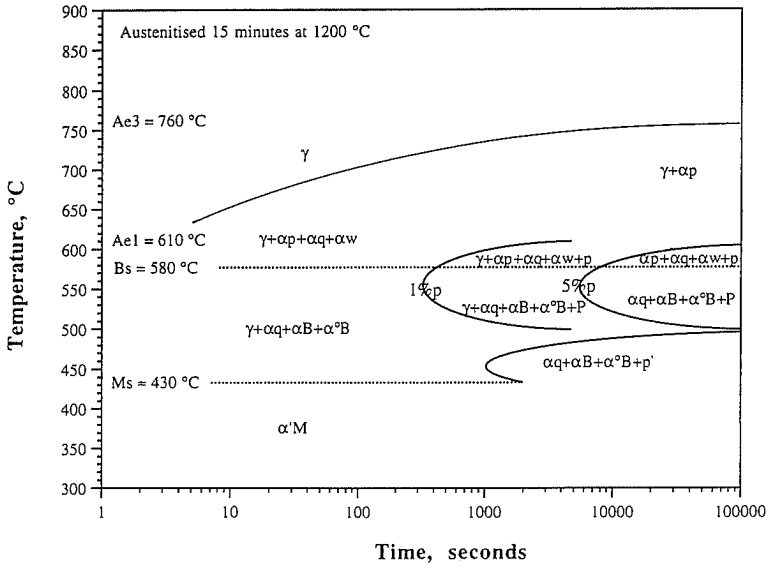

Fig. 3. Isothermal transformation diagram for HSLA80 (Table I). The notation follows the nomenclature of the Bainite Committee of the Iron and Steel Institute of Japan[45] (see Sec. 4.2): γ is austenite; αp is polygonal ferrite; αq is quasi-polygonal ferrite; p is pearlite; αB is granular bainitic; $\alpha°B$ is bainitic ferrite; p′ is degenerate pearlite; and $\alpha'M$ is lath martensite.

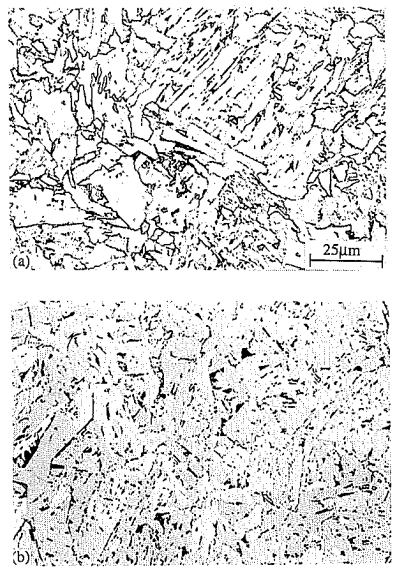

Fig. 4. Optical microstructure of bainitic structures (granular bainitic "αB" and bainitic ferrite "α°B") obtained at 480°C for 5 sec: (a) etched with nital; (b) stain etched showing martensite and/or austenite islands.

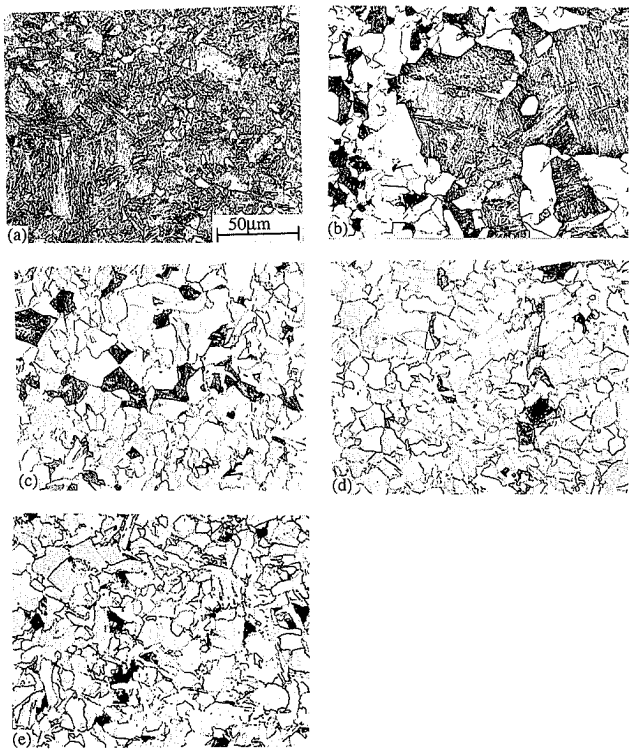

Fig. 5. Development of pro-eutectoid ferrite formation in the specimens isothermally transformed at: (a) 750°C, 8 h; (b) 635°C, 15 sec; (c) 599°C, 5 sec; (d) 599°C, 160 min; (e) 558°C, 80 min.

cluded to emphasise the carbon enrichment of austenite which accompanies ferrite formation and its effect on formation of dispersed dark islands.

3.2. Optical Microstructures

Figure 5 shows optical micrographs of microstructures observed for selected isothermal treatments. The nature of the pro-eutectoid ferrite product formed between 750 and 600°C is shown in Figs. 5(a) to 5(d). Figure 5(a) shows small ferrite grains at the boundaries of prior austenite grains in a specimen held isothermally at 750°C for 8 h. This temperature is just below Ae3. With decreasing temperature, the incubation time dropped markedly, as indicated by Fig. 5(b) for a specimen transformed at 635°C for only 15 sec. Equiaxed ferrite grains constitute nearly 50 volume percent of the structure. At 599°C for 5 sec, about 90% transformation to a quasi-polygonal type ferrite had occurred, (Fig. 5(c)). For a temperature of 599°C and 160 min (Fig. 5(d)), the microstructure consisted of 94% quasi-polygonal ferrite. Assuming that the carbon content of this ferrite is about 0.02%, the remaining austenite should contain approximately 0.52% carbon. On subsequent quenching, these austenitic regions transformed to a high carbon martensitic structure (~4%) which was darkened by stain etching (Table 2). About 2% pearlite was also present.

The extent of austenite enrichment was variable, depending on the isothermal holding time and temperature. With a decrease in transformation temperature to 558°C, the tendency for pearlite formation increased, about 4% pearlite (~94% quasi-polygonal ferrite and 2% martensite) being present afteer 80 min (Fig. 5(e)). Ferrite formed by isothermal transformation at temperatures above 600°C was mainly equiaxed at all temperatures, although the grain boundaries consisted of more planar sections as the temperature decreased and the ferrite became more quasi-polygonal. These faceted grains are a result of growth by a ledge mechanism at lower temperatures.[19–21]

Figures 6(a) and **6(c)** show micrographs of specimens isothermally transformed at 523°C for 5 sec and 80 min, respectively. The structure consists of a mixture of quasi-polygonal ferrite and lath shaped ferrite grains (granular bainitic "αB" and bainitic ferrite "α°B") associated with discrete islands or blocky regions of martensite and/or retained austenite (MA). Micro-

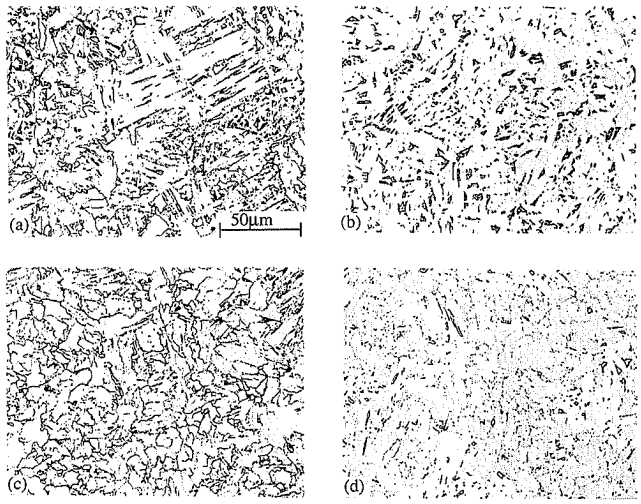

Fig. 6. Microstructural change during isothermal holding at 523°C: (a), (b) 5 sec; (c), (d) 80 min. ((a), (c) etched with nital; (b), (d) stain etched showing the corresponding MA islands).

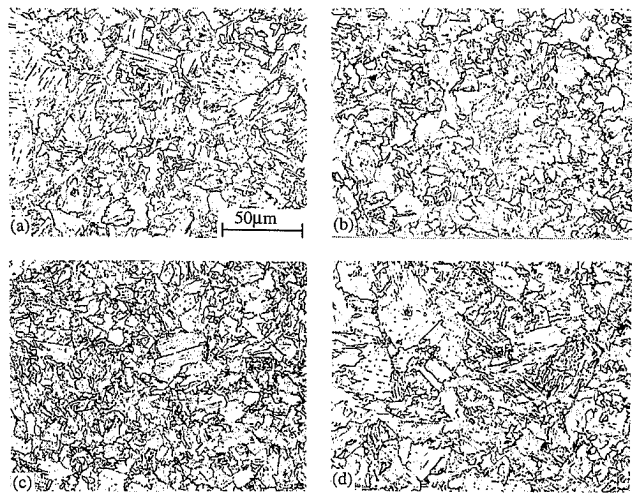

Fig. 7. Microstructures of specimens isothermally transformed at: (a) 480°C, 5 sec; (b) 480°C, 80 min; (c) 440°C, 5 sec; (d) 440°C, 40 min.

graphs of the MA islands are shown in **Figs. 6(b)** and **6(d)**. After 80 min holding at 523°C, impingement of the laths occurred and carbon enriched austenite regions partly transformed to pearlite (Figs. 6(c), 6(d)). At temperatures just below Bs, the diffusion of carbon in both bainitic ferrite and austenite is rapid,[22] and thus carbon diffuses to untransformed austenite and this carbon enriched austenite will transform diffusionally to pearlite when the carbon is in the eutectoid concentration, and the remaining austenite decomposes to high carbon transformation products on subsequent water quenching.

Examples of microstructures isothermally transformed at 480 and 440°C are shown in **Fig. 7**. The quasi-polygonal ferrite grains and bainitic forms of ferrite are evident at both temperatures in association with minor dispersed dark islands. Although the micrographs of specimens transformed isothermally at 440°C for various periods of times showed similar microstructures to those for 480°C, the ferrite laths were finer and arranged in more well defined packets or blocks at the lower temperature.

3.3. Electron Microstructures

3.3.1. Copper Precipitates

Copper precipitation was found to occur in association with polygonal and quasi-polygonal ferrite formation in this alloy. The precipitate dispersions varied considerably between samples, within the same sample and even within the same grain. In most ferrite grains examined, where precipitates could be detected, the dispersions were apparently random in nature, as indicated in **Fig. 8**, which shows regularly spaced ε-Cu precipitates displaying the same variant of the Kurdjumov–Sachs orientation relationship.[23]

Although apparently random precipitation was often observed, the section plane can disguise the presence of planar interphase precipitation. The latter mode was confirmed in some foils, as shown in the bright field micrograph of **Fig. 9(a)** and the corresponding dark field image micrograph of an ε-Cu reflection (**Fig. 9(b)**). As can be seen, the dislocation density in the polygonal ferrite is relatively low and considerable ε-Cu precipitation is present. Many of the ε-Cu precipitates are in the same crystallographic orientation, as indicated by the dark field image. The alignment of ε-Cu precipitates in the form of planar sheets parallel to the prior ferrite/austenite interface, is consistent with the interphase precipitation mode of transformation.[24–26]

3.3.2. Development of Bainitic Structures during Isothermal Transformation

(1) Transformation at 480°C for 5 sec

As the isothermal transformation temperature decreased to 580°C, the shape of the ferrite grains became much more irregular and contained a "vein" or subgrain structure (Fig. 5). Below 580°C, the ferrite grains assumed lath or plate shapes (Fig. 6) associated with bainitic transformation processes. **Figure 10** shows bright field micrographs taken from a specimen transformed isothermally at 480°C for 5 sec. Consistent with observations from optical microscopy (Fig. 4), TEM micrographs showed ferritic crystals of a lath or plate shape with a dislocation substructure. Dark regions were also located between the ferrite laths and/or packets.

Figure 11 shows a martensite/austenite (MA) island, which is representative of many similar observations of dark regions in the specimens isothermally transformed at intermediate temperatures (580–430°C) for a short period of time (5 sec). Figure 11(b) is the corresponding dark field (DF) image of an austenite reflection. The retained austenite is located at the rim of the martensite as shown in the dark image micrograph (Fig. 11(b)). The orientation relationship between the martensite and austenite shown by the electron diffraction pattern (Figs. 11(c), 11(d)) is close to the Kurdjumov–Sachs (K–S)[23] relationship.

A considerable portion of the island structure shown in Fig. 10 consisted of lath martensite, but twinned martensite was also observed in other regions. Examples of twinned martensite are shown in **Fig. 12**. Fine transformation twins are normally associated with higher carbon plate martensite and could indicate a significant enrichment of carbon in the austenite in this case. Although the exact level of carbon is difficult to determine, the observation of twinned martensite is usually considered to indicate the carbon level is

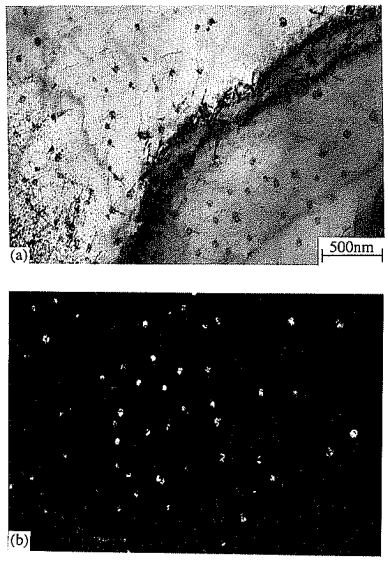

Fig. 8. Apparently random interphase ε-Cu precipitates in association with ferrite formation. Specimen isothermally transformed at 644°C for 120 min: (a) bright field image; (b) dark field image revealing copper precipitates in the same variant of the Kurdjumov–Sachs orientation relationship.

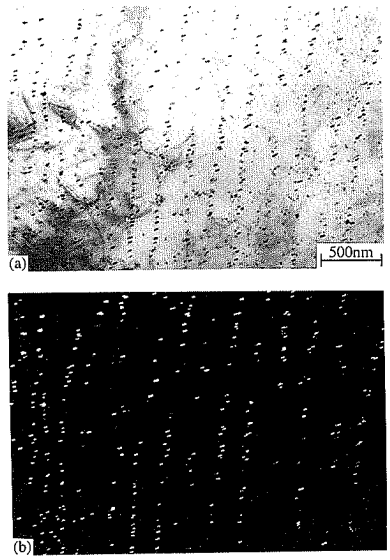

Fig. 9. Planar interphase ε-Cu precipitation in the specimen isothermally transformed at 599°C for 160 min. TEM micrographs: (a) bright field image of precipitate sheets; (b) corresponding centred dark field image from a $\{111\}_{\varepsilon\text{-Cu}}$ reflection.

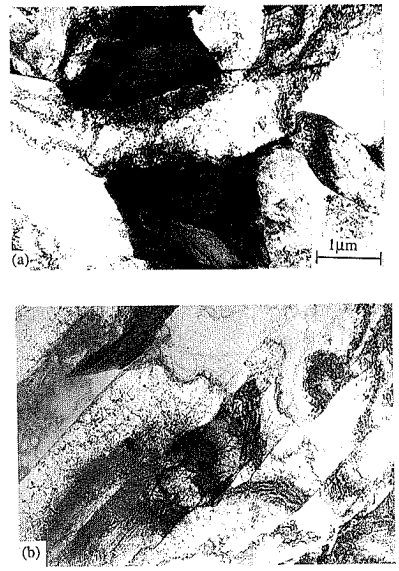

Fig. 10. TEM bright field micrographs showing the nature of dark regions in association with bainitic structures. Specimen isothermally transformed at 480°C for 5 sec: (a) granular bainitic "αB"; (b) bainitic ferrite "α°B".

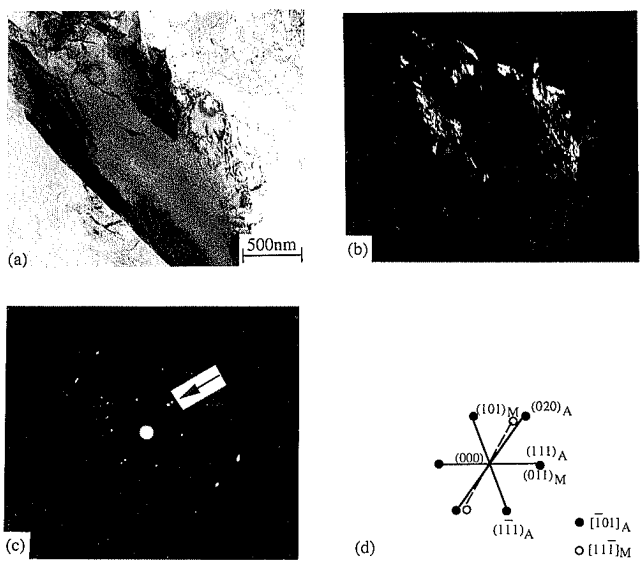

Fig. 11. Bainitic ferrite structure in association with martensite and/or austenite (MA) regions in the specimen isothermally transformed at 480°C for 5 sec. TEM micrographs: (a) bright field image showing MA constituent; (b) dark field image using $(020)_A$ austenite reflection indicated in (c); (c) corresponding diffraction pattern revealing both martensite and austenite reflections; (d) indexed pattern of some martensite (M) and austenite (A) reflections.

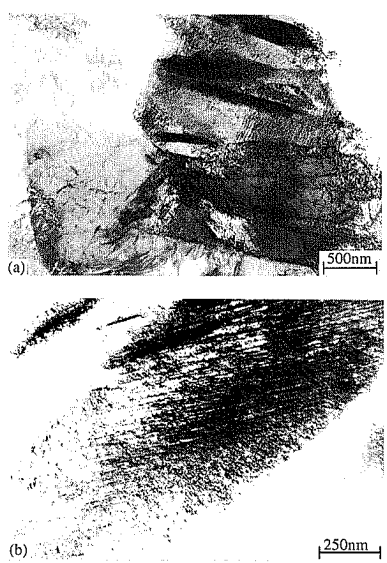

Fig. 12. Details of dispersed dark islands in the specimen isothermally transformed at 480°C for 5 sec. TEM bright field micrographs: (a) mixture of dislocated and twinned martensites; (b) twinned martensite plate.

greater than 0.4% C.[29]

An attempt was made to identify the orientation relationship between the bainitic ferrite laths and the martensite in adjacent MA islands. **Figure 13** shows an island of dislocated martensite with internal microtwins. The martensitic region adjacent to the bainitic ferrite does not show any visible microtwins. Instead, there is a dislocation network, as shown in the bright field micrograph of Fig. 13(a) and the corresponding dark field image based on $(0\bar{1}1)_M$, (Fig. 13(b)). The zone axis of the crystal orientation of the bainitic ferrite was $[311]_B$ (Figs. 13(c), 13(d)), and the adjacent martensite region exhibited a $[\bar{3}\bar{1}\bar{1}]_M$ axis, sharing a $(\bar{1}12)_M$ plane with the bainite lath (Figs. 13(e), 13(f)). In fact, the pattern of Fig. 13(e) shows that the dislocated martensite is twin related to the adjacent bainitic ferrite lath across a $(\bar{1}12)_{B/M}$ mirror plane. Moreover, the orientation of the twins within the twinned martensite is close to that of the bainitic ferrite, since both show contrast in the dark field image based on $(01\bar{1})_B$, (Fig. 13(g)). Therefore, twinning in the martensite island also occurred on $(\bar{1}12)_M$. Cementite reflections were also detected (Figs. 13(e), 13(f)), and the dark field

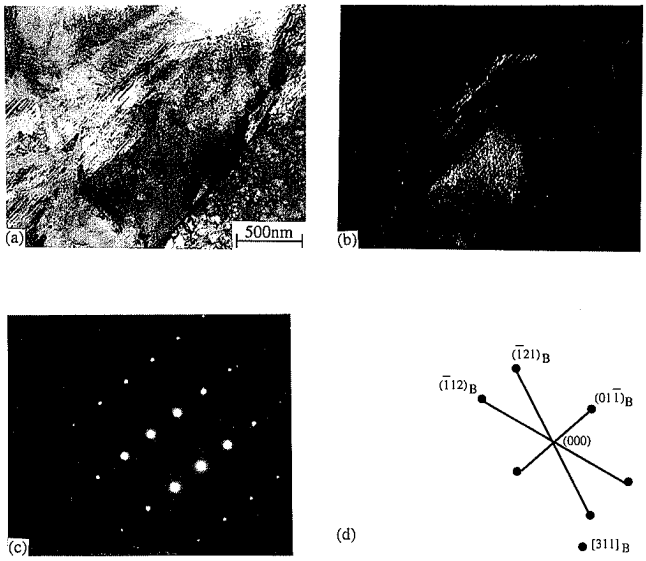

Fig. 13. Details of crystallographic orientation relationship developed between MA regions and bainitic laths in specimen isothermally transformed at 480°C for 5 sec. TEM micrographs: (a) bright field image showing a large martensite island revealing both internally twinned area and a dislocated region adjacent to the bainitic lath (lower right); (b) dark field image using dislocated martensite reflection; (c) selected area diffraction (SAD) pattern taken from bainite lath; (d) the interpretation of (c).

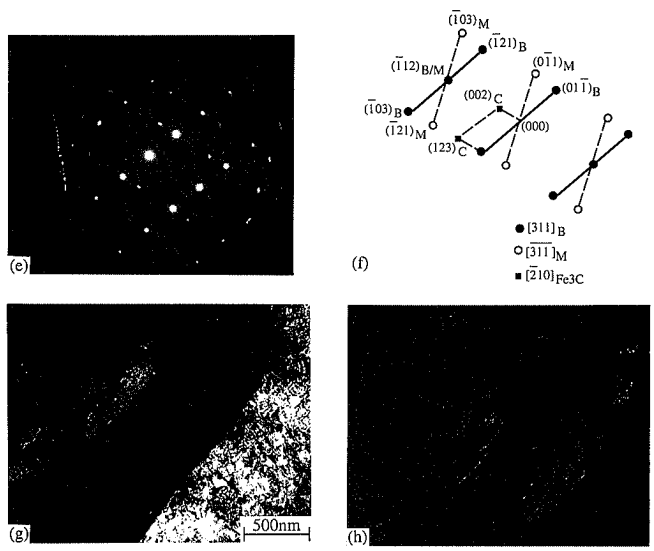

Fig. 13. Continued; (e) SAD pattern from an area which overlaps that of the bainite lath and adjacent martensite region; (f) the interpretation of (e); (g) dark field image using bainite reflection showing contrast in bainite lath and twinned martensite regions; (h) dark field image using cementite reflection.

image in Fig. 13(h) shows fine precipitates within both dislocated and twinned martensites. The orientation relationship between the orthorhombic cementite and martensite (Figs. 13(e) and 13(f)) was: $[\bar{2}10]_C//[\bar{3}\bar{1}\bar{1}]_M$, and $(002)_C//(\bar{1}12)_M$ which corresponds to one of the variants of the Bagaryatskii orientation relationship between ferrite and cementite.[30]

Twin related martensite laths have been reported in as quenched low carbon low alloy steels.[31-33] The existence of twin related laths is usually interpreted as a result of cooperative "back to back" growth of adjacent

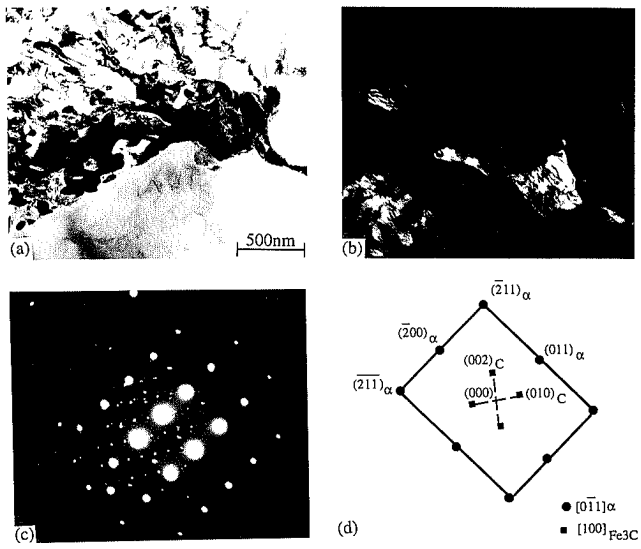

Fig. 14. Large connected cementite particles in association with the decomposition of a pool of carbon enriched austenite. Specimen isothermally transformed at 480°C for 80 min. TEM micrographs: (a) bright field image; (b) dark field image taken from cementite reflection; (c) selected area diffraction pattern showing both ferrite and cementite reflections; (d) schematic representation of (c).

laths exhibiting opposite shape deformations, *i.e.*, self accommodation.[34-36] Layers of retained austenite have been found to exist along the boundaries of adjacent laths of essentially the same orientation,[35-37] but the reported absence of such layers along the boundaries between adjacent twin related laths has been considered to support the concept that the laths form by self accommodation.[35,36] Therefore, based on the microstructural characterisation (particularly the absence of retained austenite film between the dislocated martensite region and the adjacent bainitic lath (Figs. 13(a), 13(b))) and crystallographic examination of the martensitic region with its adjacent bainitic lath (Figs. 13(e), 13(f)), it is reasonable to conclude that, under the constraints induced in the untransformed austenite by the shear and extensive strains accompanying formation of bainite laths, the carbon enriched austenite would prefer to transform martensitically to a twin related "ferrite" region, since this path is expected to minimise the accommodation strain energy for the formation of the two adjacent plate shaped crystals of ferrite.[38]

(2) Transformation at 480°C for 80 min

For a longer time of 80 min at 480°C, some carbide precipitation was visible in the microstructure. **Figures 14(a)** and **14(b)** are bright field (BF) and dark field (DF) micrographs which reveal the presence of large connected carbide particles within a ferrite matrix. It is inferred that the carbide precipitates, together with ferrite, formed from a pool of austenite during isothermal holding. The morphology of the carbide is not unlike that formed in degenerate pearlite and indicates formation by coupled growth with ferrite. **Figures 14(c)** and **14(d)**, the corresponding SADP and its schematic representation, indicate that the carbides are cementite. The orientation relationship between the orthorhombic cementite and ferrite (Figs. 14(c) and 14(d)) was verified to correspond

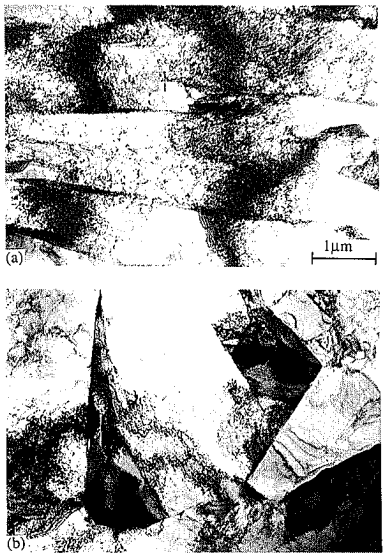

Fig. 15.
TEM bright field micrographs revealing bainitic ferrite "α°B" structure in two distinct forms. Specimen isothermally transformed at 440°C for 5 sec: (a) well developed boundaries between bainitic laths (packet A); (b) elongated martensite and/or austenite regions in a relatively non-acicular ferrite matrix (packet B).

to one of the variants of the Bagaryatskii orientation relation between ferrite and cementite.[30] The cementite precipitates are mostly in the same crystallographic orientation since most of them show contrast in the dark field micrograph. On the other hand, if cementite and ferrite independently formed from carbon enriched austenite regions, there should be multivariants of the orientation relationship between ferrite and cementite.[39] Therefore, based on the microstructral observations and crystallographic examination of the carbide, it is evident that the carbon enriched austenite region at least partly decomposed to the transformation products by cooperative growth of ferrite and cementite.

(3) Transformation at 440°C

With a further decrease in transformation temperature, both the thermodynamic driving force and the rate of the transformation will be increased resulting in a bainitic ferrite structure with the dispersed minor dark regions. **Figure 15** shows a bainitic microstructure obtained isothermally at 440°C for 5 sec. The structure consist of bainitic ferrite in two distinct forms, one with well developed boundaries separating parallel bainitic laths (packet A), and the other with dark islands between adjacent ferrite crystals (packet B). The packet A type is easily distinguishable because of the presence of subboundaries due to the slight crystallographic misorientation (about 1 or 2°) between the ferritic subunits. Therefore, the ferrite crystals in packet A are clearly "acicular", but in packet B, in many cases, the "acicularity" of the ferrite can only be inferred from the morphology and alignment of dark regions.

For this treatment, although the diffusion of carbon and alloying elements in both bainitic ferrite and austenite is slower than at 480°C, the dispersed islands contain almost the same microconstituents as those obtained at 480°C for 5 sec. **Figure 16** shows the structure of an enlarged island, which reveals an internally twinned martensite plate with carbides, precipitated on the twin–matrix interfaces. The selected area diffraction pattern shows the matrix to have $[011]_M$ zone axis and the twins to be $[0\bar{1}\bar{1}]_T$, indicating that the twinning occurs on the $(\bar{2}11)_{M/T}$ plane. It has been reported that in the presence of twins in high carbon steels, the

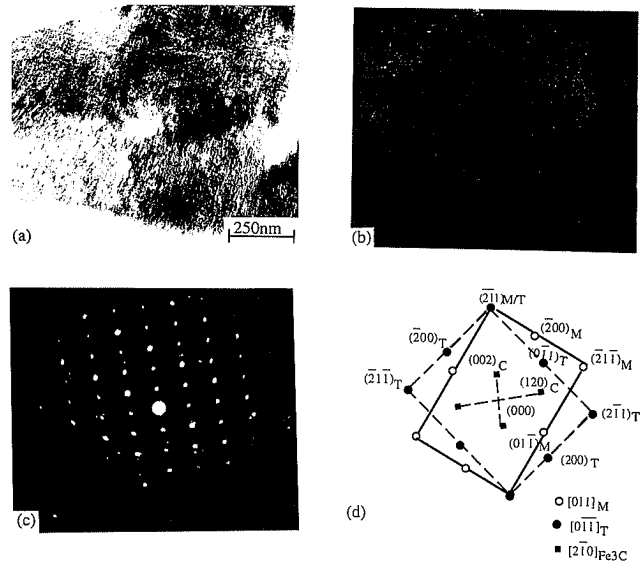

Fig. 16. Details of dispersed dark regions in the specimen isothermally transformed at 440°C for 5 sec. TEM micrographs: (a) bright field image showing internally twinned martensite; (b) dark field image based on the carbide reflection indicating cementite precipitates on the twin–matrix interfaces; (c) corresponding selected area diffraction pattern; (d) schematic representation of diffraction pattern.

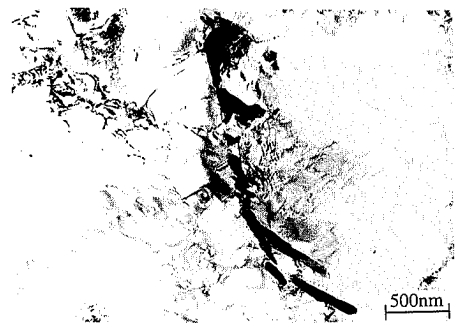

Fig. 17. TEM bright field micrograph taken from a specimen isothermally transformed at 440°C for 40 min, revealing carbide platelets formed in association with the decomposition of a pool of carbon enriched austenite.

cementite precipitates predominantly on the twin boundaries.[40] The observation of fine cementite precipitates along twin–matrix interfaces in the dark regions in this case indicates rapid autotempering of the high carbon martensite formed on quenching of untransformed austenite between the bainitic ferrite laths and/or lath packets.

No visible interlath or intralath carbide precipitation was observed in the microstructure obtained isothermally at 440°C for 5 sec. However, carbide platelet precipitation was found in the specimen transformed for a longer time. **Figure 17** shows the nature of the carbide formed by decomposition of untransformed carbon-enriched austenite after being transformed isothermally at 440°C for 40 min.

4. Discussion

4.1. Precipitation of ε-Cu

Observation of thin foils indicated that there was a

significant variation in copper precipitate morphology within the same specimen and often within the same grain. The majority of grains, where precipitate could be detected, exhibited an apparently random distribution of ε-Cu precipitates (Fig. 8). However, examination of centred dark field (CDF) and bright field (BF) images revealed that most of the precipitates displayed a single dominant variant of the K–S orientation relationship (Fig. 8). This copper precipitation morphology is analogous to the interphase precipitation of carbides found in low alloy steels containing strong carbide forming elements,[21,59] and has been termed "coherent interphase precipitation" by Honeycombe.[26]

It has been well established[25–27] that such regularly spaced sheets of precipitate are associated with the lateral movement of ledges along a low energy interface which implies a Kurdjumov–Sachs orientation relationship[23] between austenite and ferrite, and a $\{111\}_\gamma/\{110\}_\alpha$ interfacial plane. The presence of this type of precipitation has been reported in association with the formation of polygonal and quasi-polygonal ferrite[25,26] as well as the growth of Widmanstätten ferrite plates.[26,28] For the case of Widmanstätten ferrite formation, the interphase precipitation can develop during the ledge growth of the plates with the planar sheets of precipitates closely parallel to the broad faces of the Widmanstätten ferrite plates.[26,28]

Copper precipitate dispersions were also observed which appeared to be formed in accordance with the planar interphase precipitation model (Fig. 9). Large numbers of ferrite grains had to be examined to find grains favourably oriented so that the precipitate sheet morphology characteristic of interphase precipitation could be observed. A sheet precipitate morphology can readily appear to be a random dispersion in untilted foils as a consequence of grain orientation and only for certain foil orientations will the sheet morphology be obvious. In this precipitate morphology, the copper precipitate sheets were regularly spaced and generally planar, consistent with precipitation at a planar semicoherent austenite/ferrite interface. The precipitates were usually uniform in size and bright field and centred dark field images (Fig. 9) indicated that most of the precipitates have the same variant of the K–S orientation relationship.

In the present work, the observation of planar sheets of interphase ε-Cu precipitates, implies that the precipitates formed on the low energy immobile austenite/ferrite interfaces which are considered to grow *via* a ledge mechanism. This provides further supporting evidence that the dominant quasi-polygonal ferrite grains (faceted grains) formed at these relatively low temperatures grew mainly by the movement of ledges along immobile low energy phase boundaries (Fig. 5).

As the transformation temperature approached the intermediate transformation zone between those of polygonal/quasi-polygonal ferrite and martensite (580–430°C), interphase copper precipitation was not detected within the isothermally formed ferrite. However, fine uniformly distributed ε-Cu precipitates in multiple variants of the K–S orientation relationship were observed after aging, as described elsewhere[60] for bainitic samples aged under various conditions. The multivariant dispersions of copper precipitates were distinctly different from the coarse interphase precipitates observed at higher transformation temperatures. It is evident that the multivariant dispersion of copper precipitates formed from supersaturated bainitic structures formed at relatively low transformation temperatures (580–430°C).

4.2. Characteristics of Intermediate Transformation Products

Examination of the time-temperature-transformation characteristics of austenite in the low carbon, HSLA80 plate steel has shown that the austenite transforms over a wide temperature range to transformation products intermediate between those of diffusional controlled products (polygonal/quasi-polygonal ferrite and pearlite) and the low temperatue diffusionless product (martensite) (Fig. 3). Upper and lower bainite in medium carbon low alloy steels have been the first characterised intermediate microstructures[41]: upper bainite forms at temperatures below those where polygonal ferrite and pearlite form, and lower bainite forms at temperatures close to the Ms. The classical definition describes upper bainite as regions of parallel ferrite laths with interlath cementite, and lower bainite as plates of ferrite with intraplate cementite particles. Using these descriptives of bainite, the intermediate microstructures observed in this study are not easy to classify as either upper or lower bainite.

Based on the overall TEM investigation, the intermediate structures obtained in this work are characterised by a ferritic matrix consisting of lath and/or plate shaped crystals with a high dislocation density and associated with dispersed dark interlath and/or interpacket regions of martensite and/or retained austenite (Figs. 10, 15). Large packets of ferritic crystals with almost the same crystallographic orientation were often observed within prior austenite grains. In some cases, the low angle boundaries between adjacent crystals were readily observed (Figs. 10(b), 15(a)), but in other cases, there was little evidence of boundaries between the ferritic crystals, other than the presence of elongated dark regions of martensite and/or austenite formed from pools of untransformed austenite on quenching (Fig. 15(b)). The low-angle boundaries between the ferritic crystals are insensitive to etching, and as such, little or no evidence of interlath boundaries was detected by optical microscopy. Therefore, the optical microstructure is characterised by the appearance of dispersed dark regions in a relatively featureless matrix. In fact, the microstructure consists of martensite and/or austenite islands located between the packets of lath and/or plate shaped ferritic crystals.

There has been a considerable discussion about the morphological features of ferritic microstructures formed at intermediate temperatures and cooling rates in low carbon low alloy steels.[42–45] On the basis of isothermal transformation studies on low carbon low alloy steels, Ohmori *et al.*[46] concluded that three morphological forms of bainite can occur. These are: carbide-free bainite occurring in the temperature range 600–500°C (BI); conventional upper bainite at 525–450°C (BII); and lath type lower bainite at 450–400°C (BIII). The results of the present investigation are consistent with the formation of carbide-free bainitic structure (BI).

Habraken[47] and Economopoulos *et al.*[42] proposed that the microstructure of ferrite with islands of martensite/austenite (MA) should be referred to as granular bainite, because of the "granular" appearance of the MA islands in the matrix. An attempt was made by Bramfitt and Speer[43] to summarise the morphological features of structures in low carbon ferritic steels and they classified a microstructure consisting of an acicular (carbide-free) ferrite associated with a constituent consisting of discrete islands or blocky regions (of austenite and/or martensite, or pearlite) as B_3 type bainite.

Krauss and Thompson have chosen the terms acicular ferrite "AF" and granular ferrite "GF" to describe the unique microstructural features in low carbon microalloyed steels undergoing both isothermal and continuous cooling transformations, and these terms are considered to emphasise that the austenite transforms only to a single phase ferrite with lath and/or non-lath morphologies, respectively.[44,48] As pointed out by Bhadeshia however,[49,50] the use of the term "acicular ferrite" in this context is apt to be confusing and the label, acicular ferrite, should be reserved for the intragranular product formed in association with inclusions in coarse grains of austenite in weld metals or in oxide inoculated hot rolled steels.

The Bainite Committee of the Iron and Steel Institute of Japan (ISIJ)[45] has also offered a classification for ferritic transformation products in modern HSLA steels. The ISIJ nomenclature is based on the detailed observations of the structures of low carbon microalloyed steels transformed under defined conditions following hot rolling or normalising. The Japanese classification (see caption to Fig. 3) uses the terms granular bainitic "αB" and bainitic ferrite "α°B" to describe the most common bainitic type structures formed in low carbon steels and these terms are considered to be the most appropriate descriptions for the bainitic structures observed in this investigation.

4.3. Characteristics of Dispersed Dark Regions

It was observed that the martensitic structure is the dominant microconstituent of the dark regions in the specimens isothermally transformed at intermediate temperatures (580–430°C) for a short period of time (5 sec) (Figs. 12, 13, 16). The martensitic products formed in steel can generally be differentiated by the transformation substructure: twinned substructure (plate martensite) and dislocated substructure (lath martensite),[51] with these morphologies depending primarily upon the carbon content.[52–54] Typically, plate martensite is produced in high carbon alloys containing more than 0.8% carbon,[53,54] while lath martensite is formed in low carbon alloys with less than about 0.2% carbon.[53] Alloys with intermediate compositions will exhibit both martensite morphologies. Based on the overall TEM investigation, it is evident that a twinned substructure is present in a significant volume fraction of dark regions in the specimens isothermally transformed at intermediate temperatures for a short period of time (Figs. 12, 13, 16). The volume fraction of dark regions in the specimen isothermally transformed at 480°C for 5 sec (Figs. 4(a), 4(b)) is about 5% and the average carbon content for the regions is calculated to be about 0.6%. According to work carried out by Speich,[55] the quenched structure of a steel containing 0.45–0.55% C should be typically lath martensite with about 20% twinned substructure.[55] Therefore, the level of carbon partitioning of dark regions formed on quenching in the specimens isothermally transformed at intermediate temperatures in the specimens isothermally transformed at intermediate temperatures is in good agreement with those higher carbon martensitic structures studied by Speich.[55]

In the present work, the bainitic structures obtained by isothermal transformation at intermediate temperatures consisted of parallel bainitic ferrite laths or plates in association with interlath and/or interpacket dark regions. The dispersed martensitic islands formed from carbon enriched residual austenite on quenching after isothermal transformation mainly at intermediate temperatures for relatively short holding times (5 sec). For longer holding times, the carbon enriched austenite regions decomposed to carbide platelets and ferrite by coupled growth prior to quenching.

The dark regions were identified by TEM micrographs and diffraction patterns as the martensite/austenite (MA) constituent, untempered lath and twinned martensite, autotempered twinned and dislocated martensite, and ferrite containing cementite particles, depending on the level of carbon supersaturation of the austenite and the transformation temperature and time. The ferritic structures formed over the temperature range of 580–430°C are consistent with the carbide-free bainitic structures reported by several investigators[56–58] for low carbon steels.

5. Conclusions

A study of the isothermal, subcritical transformation of austenite in a low carbon (0.05% C) CR HSLA80 plate steel, containing significant additions of manganese, copper, and nickel, produced the following conclusions.

(1) The austenite transformed to ferritic microstructures with morphologies and substructures which are a function of transformation time and temperature. Polygonal ferrite and quasi-polygonal ferrite formed at relatively high transformaton temperatures and these structures were characterised by low dislocation densities and contained ε-copper precipitates formed by an interphase transformation mechanism. The presence of ε-copper precipitates provides evidence for long-range substitutional atom diffusion during high temperature ferrite formation, as well as transformation of austenite by a ledge mechanism.

(2) At intermediate transformation temperature (580–430°C), the microstructure was characterised predominantly by parallel ferrite laths with a high density of dislocations, which have similar crystallographic orientations within each packet. Interlath and/or interpacket dark regions were present which resulted from transformation of pools of retained austenite either at temperature or on quenching. For a short holding time (5 sec), the dark regions were identified as the mixed martensite/austenite (MA) constituent, autotempered twinned and lath martensite, and untempered twinned and lath martensite, depending on the level of carbon partitioning in the remaining austenite regions before quenching in water.

(3) The martensite and austenite in the MA constituent showed the K–S orientation relationship.

(4) Dislocated lath martensite formed in carbon enriched austenite islands exhibited a twin relationship with its adjacent bainitic ferrite lath.

(5) Fine carbides which formed by autotempering were observed on martensite twin boundaries within the MA constituent and showed an orientation relationship with the martensitic ferrite consistent with a variant of the Bagaryatskii relationship.

(6) Coarser carbide platelets formed in remaining austenite pools during prolonged holding at temperatures in the range 480–440°C. The nature of the carbide and its crystal orientation indicated that decomposition of austenite had occurred by coupled growth of ferrite and carbide.

Acknowledgments

One of the authors (S. S. Ghasemi Banadkouki) is grateful to the Ministry of Culture and Higher Education of I. R. Iran for providing a scholarship, and to Dr. D. Wexler for helpful TEM discussions at the University of Wollongong. The support of BHP Steel, SPPD, Port Kembla, in provision of material and technical information is gratefully acknowledged.

REFERENCES

1) A. D. Wilson: *J. Met.*, **39** (1987), No. 3, 36.
2) M. R. Krishnadev and I. LeMay: *J. Iron Steel Inst.*, **208** (1970), 458.
3) M. Es-Souni and P. A. Beaven: *Mater. Sci. Eng.*, **A130** (1990), 173.
4) Y. Kohsaka and C. Ouchi: *ATB Metall. (Acta Technica Belgica)*, **23** (1983), No. 3, 9.1.
5) E. Hornbogen and R. C. Glenn: *Trans. TMS-AIME*, **218** (1960), 1064.
6) H. Wada, Y. Houbaert, J. Penning and J. Dilewijns: *ATB Metall. (Acta Technica Belgica)*, **23** (1983), No. 3, 3.1.
7) J. Y. Yoo, W. Y. Choo, T. W. Park and Y. W. Kim: Int. Symp. on New Aspects of Microstructures in Modern Low Carbon High Strength Steels, Tokyo, Japan, (1994), 83.
8) P. Wacquez and R. V. Daehle: *Sheet Met. Ind.*, **44** (1967), No. 477, 21.
9) I. LeMay and L. M. Shetky: Copper in Iron and Steel, John Wiley and Sons, New York, (1982).
10) I. LeMay: *J. Met.*, **6** (1971), No. 2, 436.
11) T. W. Montemarano, B. P. Sack, J. P. Gudas, M. G. Vassilaros and H. H. Vanderveldt: *J. Ship Production*, **2** (1986), No. 3, 145.
12) J. C. West: *J. Ship Production*, **3** (1987), 111.
13) L. F. Porter and P. E. Repas: *J. Met.*, **34** (1982), No. 4, 14.
14) T. Abe, M. Kurihara, H. Tagawa and K. Tsukada: *Trans. Iron Steel Inst. Jpn.*, **27** (1987), 478.
15) L. G. Kvidahl: *Weld. J.*, **64** (1985), 42.
16) T. Gladman and J. H. Woodhead: *J. Iron Steel Inst.*, **194** (1960), 189.
17) J. E. Hilliard and J. W. Cahn: *Trans. AIME*, **221** (1961), 344.
18) K. W. Andrews: *J. Iron Steel Inst.*, **203** (1965), 721.
19) K. R. Kinsman and H. I. Aaronson: *Metall. Trans.*, **4** (1973), 959.
20) K. R. Kinsman, E. Eichen and H. I. Aaronson: *Metall. Trans. A.*, **6A** (1975), 303.
21) R. W. K. Honeycombe: *Metall. Trans. A*, **7A** (1976), 915.
22) H. Ohtani, S. Okaguchi, Y. Fujishiro and Y. Ohmori: *Metall. Trans. A*, **21A** (1990), 877.
23) G. Kurdjumov and G. Sachs: *Z. Physik*, **64** (1930), 325.
24) R. A. Ricks, P. R. Howell and R. W. K. Honeycombe: *Met. Sci.*, **14** (1980), 562.
25) K. Campbell and R. W. K. Honeycombe: *Met. Sci. J.*, **8** (1974), 197.
26) R. A. Ricks, P. R. Howell and R. W. K. Honeycombe: *Metall. Trans. A*, **10A** (1979), 1049.
27) H. I. Aaronson, M. R. Plichta, G. W. Franti and K. C. Russell: *Metall. Trans. A*, **9A** (1978), 363.
28) P. R. Howell, R. A. Ricks and R. W. K. Honeycombe: *J. Mater. Sci.* **15** (1980), 376.
29) C. Speich: Metals Handbook, Vol. 8, 8th Ed., Metallography, Structure and Phase Diagrams, ASM, Ohio, (1973), 197.
30) Y. A. Bagaryatskii: *Akad. Nauk. SSSR*, **73** (1950), 1161.
31) G. R. Speich and H. Warlimont: *J. Iron Steel Inst.*, **206** (1968), 385.
32) S. K. Das and G. Thomas: *Metall. Trans.*, **1** (1970), 325.
33) B. V. N. Rao, R. W. Miller and G. Thomas: Proc. 16th Int. Heat Treatment Conf., The Metals Society, London, (1976), 75.
34) G. R. Speich and P. R. Swann: *J. Iron Steel Inst.*, **203** (1965), 480.
35) B. V. N. Rao and G. Thomas: Proc. Int. Conf. on Martensite Transformation, Cambridge, MA, (1979), 12.
36) H. K. D. H. Bhadeshia and D. V. Edmonds: Proc. Int. Conf. on Martensite Transformation, Cambridge, MA, (1979), 28.
37) K. Wakasa and C. M. Wayman: *Acta Metall.*, **29** (1981), 991.
38) H. K. D. H. Bhadeshia: *Acta Metall.*, **29** (1981), 1117.
39) J. L. Lee, S. C. Wang and G. H. Cheng: *Mater. Sci. Technol.*, **5** (1989), 674.
40) D. H. Huang and G. Thomas: *Metall. Trans.*, **2** (1971), 1587.
41) E. S. Davenport and E. C. Bain: *Trans. AIME*, **90** (1930), 117.
42) M. Economopoulos and L. J. Habraken: Transformation and Hardenability in Steels, Climax Molybdenum Company, Ann Arbor, MI, (1967), 69.
43) B. L. Bramfitt and J. G. Speer: *Metall. Trans. A*, **21A** (1990), 817.
44) G. Krauss and S. W. Thompson: Int. Symp. on New Aspect of Microstructures in Modern Low Carbon High Strength Steels, Tokyo, (1994), 1.
45) T. Araki: Atlas for Bainitic Microstructures Vol. 1, Bainite Committee of Iron and Steel Inst. of Japan, (1992).
46) Y. Ohmori, H. Ohtani and T. Kunitake: *Trans. Iron Steel Inst. Jpn.*, **11** (1971), 250.
47) L. J. Habraken: Proc. 4th Int. Conf. on Electron Microscopy, Springer-Verlag, Berlin, (1960), 621.
48) S. W. Thompson, D. J. Colvin and G. Krauss: *Metall. Trans. A*, **21A** (1990), 1493.
49) S. S. Babu and H. K. D. H. Bhadeshia: *Mater. Trans., JIM*, **32** (1991), No. 8, 679.
50) H. K. D. H. Bhadeshia: Bainite in Steels, Microstructures and Properties, The Inst. of Metals, London, (1992), 245.
51) G. Krauss and A. R. Marder: *Metall. Trans.*, **2** (1971), 2343.
52) P. M. Kelly and J. Nutting: *J. Iron Steel Inst.*, **197** (1961), 199.
53) G. R. Speich and W. C. Leslie: *Metall. Trans.*, **3** (1972), 1043.
54) G. Krauss: Steels: Heat Treatment and Processing Principles, ASM Int., Metals Park, OH, (1990), 52.
55) G. R. Speich: *Trans. AIME*, **245** (1969), 2553.
56) S. W. Thompson, D. J. Colvin and G. Krauss: *Sci. Metall.*, **22** (1988), No. 7, 1069.
57) J. L. Lee, M. H. Hon and G. H. Cheng: *Scr. Metall.*, **21** (1987), No. 3, 293.
58) Z. Bojarski and T. Bold: *Acta Metall.*, **22** (1974), 1223.
59) R. A. Ricks and P. R. Howell: *Acta Metall.*, **31** (1983), 853.
60) S. S. G. Banadkouki, D. Yu and D. P. Dunne: to be published in *ISIJ Int.*